New Ethyl Cellulose/Acrylic Hybrid Latexes and Coatings via Miniemulsion Polymerization

R. CHEN,[1,2] F. CHU,[2] C. GAUTHIER,[3] L. CHAZEAU,[3] I. CHADUC,[1] E. BOURGEAT-LAMI,[1] M. LANSALOT[1]

[1]Université de Lyon, Univ. Lyon 1, CPE Lyon, CNRS UMR 5265, Laboratoire de Chimie, Catalyse, Polymères et Procédés (C2P2), LCPP group, 43 Bd. du 11 Novembre 1918, F-69616, Villeurbanne, France

[2]Institute of Chemical Industry of Forest Products, Chinese Academy of Forestry, 16 Suo Jin Wucun, 210042 Nanjing, China

[3]MATEIS, INSA-Lyon, 7 avenue Jean Capelle, F-69621 Villeurbanne Cedex, France

Received 21 December 2009; accepted 26 February 2010
DOI: 10.1002/pola.23998
Published online in Wiley InterScience (www.interscience.wiley.com).

ABSTRACT: Ethyl cellulose (EC) was incorporated into copolymer latexes via miniemulsion polymerization. The effects of EC viscosity and EC content on droplet size, particle size, and polymerization kinetics were investigated. The higher the EC content and viscosity, the larger the droplet size and the less stable the latex suspension. Small droplets that could be efficiently nucleated were formed for the lower-viscosity EC but the latex still showed limited colloidal stability. This was attributed to some phase-incompatibility between EC and the acrylic polymer. These stability issues were overcome by using an oil-soluble initiator and a crosslinker. The later enabled to physically entrap EC inside the polymer particles, whereas the former allowed in situ grafting of the growing acrylic radicals to the EC backbone decreasing thereby the extent of phase separation. Thermal-mechanical analyses evidenced that the films obtained from the hybrid latexes displayed better properties than the EC-free latex films or the physical blends. This supports the hypothesis of formation of hybrid latexes that synergistically combine the properties of the acrylic matrix and the EC polymer. Interestingly, a significant increase of the elastic modulus was observed between 50 and 90 °C. This mechanical reinforcement was tentatively attributed to the formation of a percolating EC-based hybrid phase. © 2010 Wiley Periodicals, Inc. J Polym Sci Part A: Polym Chem 48: 2329–2339, 2010

KEYWORDS: acrylic; ethyl cellulose; hybrid latexes; mechanical properties; miniemulsion polymerization; phase incompatibility

INTRODUCTION Cellulose is an abundant natural polymer with renewable and biodegradable characteristics.[1] It is widely used as an additive in membranes, pharmaceuticals, and foodstuffs. Among cellulosic materials, ethyl cellulose (EC) is a chemically modified cellulose derivative, which has attracted a particular attention in recent years. This material is used in various fields such as plastics, coatings, rubbers, printing inks, and insulated materials owing to its high dielectric strength and stability with light, heat, oxygen, damp, base, and dilute acid. In addition, EC is highly compatible with phenolic resins, alkyds, and plasticizers. It also shows a low-residue on ignition after burning, contributes to film toughness without any additives, and keeps flexibility under low-temperature. At last, EC films and plastics have exceptional mechanical strength and flexibility in a wide range of temperatures.[1] The cellulose backbone of EC can be chemically modified with synthetic polymers via different polymerization techniques, such as irradiation with ultraviolet light,[2] ring-opening polymerization,[3] or atom transfer radical polymerization.[4–7] As typical examples, we can mention the synthesis of EC-graft-poly(ε-caprolactone) and their block copolymers with poly(L-lactide),[3] EC-graft-poly(ethylene glycol) allenyl methyl ether macromonomer[8] and EC-based amphiphilic copolymers with poly(acrylic acid) or poly(poly (ethylene glycol) methyl ether methacrylate pendant chains. In the field of emulsions, EC can be used as an emulsifier,[9] incorporated into coatings,[10,11] or used to elaborate microspheres notably for drug delivery applications.[12–14] The most developed procedure for the preparation of EC pseudolatexes relies on either the emulsification/solvent evaporation (ESE) process[15,16] (which consists in the dissolution of EC in a suitable solvent, its subsequent emulsification into water phase containing suitable emulsifying agent, and finally the solvent evaporation) or miniemulsification.[17] A process based on nanoprecipitation has also been reported.[18] Recently, Arias et al. synthesized core-shell particles consisting of a magnetic carbonyl iron core and a biocompatible EC shell using the ESE process.[19]

Although various cellulosic derivatives have been used for the elaboration of advanced materials for coating applications,[10,20,21] to our knowledge, there is no work reporting the incorporation of EC into polymer latex particles. In the present article, EC was incorporated into polyacrylic latexes via miniemulsion polymerization with the ultimate goal of

Correspondence to: E. Bourgeat-Lami (E-mail: bourgeat@lcpp.cpe.fr) and M. Lansalot (E-mail: lansalot@lcpp.cpe.fr)
Journal of Polymer Science: Part A: Polymer Chemistry, Vol. 48, 2329–2339 (2010)

improving the properties of the resulting polymer film materials. The choice of miniemulsion as the polymerization process was motivated by the demonstrated ability of this technique to encapsulate various hydrophobic or inorganic components inside polymer particles.[22–26] Instead of physically blending EC and the latex suspension, we thus dispersed EC into acrylic monomers, formed nanosize droplets by sonication and then polymerized the EC-containing nanodroplets. This method should not only enable achieving intimate mixing between EC and the acrylics but may also offer the opportunity to covalently link the EC to the polymer matrix. This work aimed at finding appropriate conditions to synthesize such latexes that should be colloidally stable and contain as much EC as possible. The mechanical properties of the films obtained from the hybrid latexes were compared with those of pure acrylic films.

EXPERIMENTAL

Materials

Butyl acrylate (BA, >99%, Aldrich), methyl methacrylate (MMA, 99%, Aldrich), triethylene glycol dimethacrylate (TEGDMA, 95%, Aldrich), hexadecane (HD, 99%, Acros Organics), ammonium persulfate (APS, 98%, Acros Organics), dilauroyl peroxide (LPO, 99%, Acros Organics), sodium dodecyl sulfate (SDS, 99%, Acros Organics), EC (EC, Aldrich) with viscosities of 10 and 100 cP (viscosity in 5 wt % solution of 80/20 toluene/ethanol) hereafter referred to as EC10 and EC100, respectively, were used as received. Water was deionized before use (Purelab Classic UV, Elga LabWater).

EC Characterization

Molar masses and molar mass distributions of the commercial EC samples were determined by size exclusion chromatography using a modular system comprising a Waters 515 HPLC pump and an autosampler 717Plus (Waters). A precolumn (PLgel 5 μm) and three columns [two PLgel 5 μm Mixed C (300 $\times$ 7.5 mm^2) and one PLgel 5 μm 500 Å (300 $\times$ 7.5 mm^2)] thermostated at 30 °C were used with THF as eluent at a flow rate of 1 mL·min^{-1}. Waters 410 refractometer was used for detection, and molar masses were calculated on the basis of a calibration curve using narrow polydispersity polystyrene standards. The viscosity of EC-monomer solutions was measured using a RFS III rheometer (Rheometric Scientific). The measurements were performed on ~20 g of liquid at 25 °C. The reported viscosity values were taken at the plateau.

Solution Polymerization

Polymerizations in solution were performed in a three necked round-bottom flask equipped with a condenser, a thermometer, a magnetic stirrer, and an argon inlet. The reaction vessel was loaded with a mixture of monomers (MMA/BA 50/50 by weight), EC (10 wt %/monomers), and toluene (targeted solid content = 33 wt %) and immersed in an oil bath. The mixture was degassed under argon for 30 min at room temperature while the temperature was raised to 75 °C. Finally, the introduction of LPO dissolved in toluene gave the zero time of the polymerization. Monomer consumption was followed by gravimetric analysis of samples withdrawn from the polymerization medium at different times. Molar masses and molar mass distributions of the dried polymers were calculated on the basis of a calibration curve using low polydispersity poly(methyl methacrylate) standards.

TABLE 1 General Recipe for the Miniemulsion Polymerizations of Methyl Methacrylate (MMA)/Butyl Acrylate (BA) in the Presence of Ethyl Cellulose (EC)

Organic phase	
MMA + BA + EC	20% solid content
MMA/BA	50/50 by weight
EC (wt %)[a]	5–20
TEGDMA (wt %)[a]	4.7–17
HD (wt %)[a]	6.7
LPO[b] (wt %)[a]	0.5
Water phase	
Deionized water	105 g
SDS (wt %[a])	1
APS[b] (wt %[a])	0.5

[a] With respect to monomers or monomers/EC mixture.
[b] Polymerization temperature: 80 °C with LPO, 75 °C with APS.

Latex Synthesis and Characterization

Batch miniemulsion copolymerizations were performed in a glass-jacketed reactor equipped with a condenser and a nitrogen inlet. The monomers (BA and MMA, 50/50 by weight) were first mixed with the hydrophobe, EC (if used), and the crosslinker (TEGDMA, if used). This organic phase was then added to the aqueous solution containing the surfactant (SDS) under vigorous stirring. The resulting mixture was then ultrasonicated (750 W Vibracell 75042, amplitude 90%) for 5 min. The obtained miniemulsion was next introduced into the reactor and deoxygenated by purging with nitrogen for 20 min while the temperature was raised to 75 °C. Finally, the addition of initiator (APS) gave the zero time of the polymerization. A slightly different procedure was followed when using an oil-soluble initiator. LPO was dispersed into the organic phase before the sonication step, and the polymerization was performed at 80 °C. The experimental conditions of all the polymerizations performed in this study are displayed in Tables 1 and 2.

Monomer consumption was followed by gravimetric analysis of samples withdrawn from the polymerization medium at different times. The droplet and particle sizes (hydrodynamic diameter–D_d and D_p, respectively) were measured by dynamic light scattering (Zetasizer HS1000 from Malvern Instruments), and the data were collected using the fully automatic mode of the Zetasizer system. It is worth noting that the droplet size was in each case measured straight after the preparation of the miniemulsion. The mean size distribution, Poly, is a dimensionless measure of the distribution broadness determined from the autocorrelation function using a second-order method of cumulant analysis.[27] For a monodisperse sample, the poly value should theoretically be

TABLE 2 Summary of Experimental Conditions of all the Miniemulsion Polymerizations Performed in this Study. Effects of Synthetic Parameters on Droplet Size, Particle Size, Monomer Conversion, and Weight Fraction of Coagulum

Run	EC type	EC (wt %)[a]	Initiator	TEGDMA (g)	D_d (nm)	Poly	D_p (nm)	Poly	Conversion (%)[b]	Coagulum (wt %)[c]
1		0	APS		111	0.210	109	0.017	100	0
2	EC100	5	APS		139	0.149	119	0.039	89	ND[d]
3	EC100	10	APS		219	0.148	139	0.038	82	ND
4	EC100	15	APS		354	0.595	86	0.310	74	ND
5	EC10	10	APS		143	0.161	101	0.022	68	38
6	EC10	10	APS	2.1	148	0.149	120	0.056	85	26
7	EC10	10	LPO	2.1	105	0.181	180	0.064	100	0
8		0	LPO	2.1	141	0.194	230	0.064	56	0
9	EC10	15	LPO	2.1	148	0.173	205	0.121	55	12
10	EC10	15	LPO	3.8	157	0.142	219	0.056	62	10
11	EC10	15	LPO	7.65	156	0.142	214	0.072	24	21
12	EC100	10	LPO	2.1	199	0.127	280	0.109	71	13

[a] In wt % with respect to monomers/EC mixture.
[b] Polymerization time = 90 min.
[c] Based on the total weight of polymer and EC.
[d] ND = not determined.

zero. In practice, a poly value for a "monodisperse" latex lies between 0 and 0.05. The poly value can be considered to have lost its significance for values above 0.15, but below a value of 0.5 useful comparisons between samples can be made. The number of droplets, N_d, or particles, N_p ($mL^{-1}{}_{Latex}$), was calculated using the diameter obtained from DLS (either D_d or D_p, nm) according to eq 1, with τ the solid content of the dispersed phase (comprising the monomer and polymer present for a given conversion and expressed in $g{\cdot}mL^{-1}{}_{Latex}$), and ρ ($g{\cdot}cm^{-3}$) the density of the particles (taking into account the conversion).

$$N_p, N_d = \frac{6\tau}{\rho\pi(\text{diameter})^3} \times 10^{21}. \quad (1)$$

Conductivity measurements were performed on a CDM83 conductimeter. A concentrated SDS solution (40 $g{\cdot}L^{-1}$) was added dropwise to a known volume of water in the presence of APS, and the conductivity of the solution monitored. The SDS critical micelle concentration (CMC) was determined to be 2.36 $g{\cdot}L^{-1}$ of water, in good agreement with values reported in the literature.[28] The evolution of conductivity versus SDS concentration below the CMC could be expressed as follows: Conductivity ($mS{\cdot}cm^{-1}$) = 0.44 × [SDS] ($g{\cdot}L^{-1}$) + 0.0468. This allowed us to determine the concentration of SDS in the aqueous phase for the miniemulsions.

Imaging Techniques

Transmission Electron Microscopy (TEM) analyses were carried out at the Centre Technologique des Microstructures (CTμ), Claude Bernard University, Villeurbanne, France. A drop of the diluted latex suspension was deposited on a formvar-coated copper grid and allowed to evaporate before observation at the accelerating voltage of 80 kV using a Philips CM120 microscope.

Film Formation and Film Characterizations

The film formation was carried out as follows. The desired amount of latex (10 g with 30% solid content) was first cast into a Teflon mold (8 cm in diameter), and then dried in an oven thermostated at 35 °C overnight. The film was taken out of the pan, quickly washed with distilled water to get rid of the exuded emulsifier, and dried again at 35 °C for 30 min.

The hybrid films were analyzed by differential scanning calorimetry (DSC). Appropriate amounts of samples were sealed in aluminum pans. DSC thermoscans of the materials were then recorded under a dry nitrogen atmosphere at a heating rate of 10 $°C{\cdot}min^{-1}$ from 20 to 130 °C, in two scans using a Setaram DSC 131 apparatus.

Dynamic mechanical analysis (DMA) measurements were performed on rectangular specimens (15 × 6 × 2 mm^3) with an inverted torsion pendulum apparatus already described in literature.[29] This device works in a helium atmosphere, in the temperature range of 100–700 K and frequency range of 5.10^{-5}–5 Hz. The storage (G′) and loss (G″) parts of the dynamic shear modulus, and so the internal friction tanδ (G″/G′) were measured as a function of temperature (from 173 to 373 K), with a heating rate of $1°{\cdot}min^{-1}$, and a frequency of 0.1 Hz.

RESULTS AND DISCUSSION

Characteristics of the EC Powders and of the Resulting Monomer Solutions

The physicochemical properties of EC and notably the molar mass, the ethoxyl content and the glass transition temperature (T_g) are of central importance in this study. Table 3 summarizes the experimental values determined for the two different EC grades employed in this work. It is seen that EC10 and EC100 have the same ethoxyl content and similar

TABLE 3 Physicochemical Features of EC Samples of Increasing Viscosities

EC Grade	EC10	EC100
Viscosity (cP)[a]	10	100
M_n (g·mol^{-1})	19 470	35 280
M_w (g·mol^{-1})	55 330	138 300
M_w/M_n	2.8	3.9
Ethoxyl content (%)[b]	48	49
T_g (°C)	122	128

[a] As determined by the supplier for a 5 wt % EC solution of 80/20 toluene/ethanol.
[b] According to the provider, an ethoxyl content of 48% corresponds to a degree of substitution (D.S.) of Et functionalities on the cellulose backbone in the range of 2.25–2.58 mol ethyl per mol cellulose.

T_gs' but different molar masses in agreement with the viscosity data.

As the viscosity of the monomer phase is a key factor for a successful emulsification, we investigated the effect of EC content on the viscosity of the monomer solution. To do so, increasing amounts of EC were dissolved into a 50/50 (wt/wt) MMA/BA mixture and the viscosity of the resulting solutions was determined as detailed in the experimental part. The results are reported in Table 4. As expected, the values measured for 5 wt % of both types of EC were in good agreement with the supplier data and increased with increasing EC content.

Preparation of EC-Loaded Miniemulsion Droplets

As reported in literature, the viscosity of the dispersed phase influences the droplet size of oil-in-water emulsions.[30–32] Figure 1 shows the evolution of the MMA/BA droplet size as a function of sonication time for different amounts of EC100. As expected, the droplet size decreased with increasing sonication time and increased with increasing EC content that is to say with increasing the viscosity of the EC-acrylate solution. For EC contents comprised between 5 and 15 wt %, the droplets were stable. However, for higher EC contents, we could not produce stable miniemulsion droplets even when increasing the applied power/volume ratio. Mabille et al. proposed a relationship between the droplet size, D_d, and the viscosity ratio, R, between the dispersed and continuous phase.[33] For stable miniemulsions (0–15 wt % of EC), the evolution of the droplet diameter with the viscosity ratio could be fitted with a power law, which agrees well with that of Mabille et al. $D_d = 49 \times R^{0.21}$.

TABLE 4 Viscosities of a Series of EC-Acrylate Monomer Solutions as a Function of EC Content and EC Grade

EC grade	EC10			EC100		
EC content (%)	5	10	15	5	10	15
Viscosity of EC/acrylate solution (cP)	10	100	410	120	1380	9370[a]

[a] This value should be considered with caution due to the high viscosity of the solution.

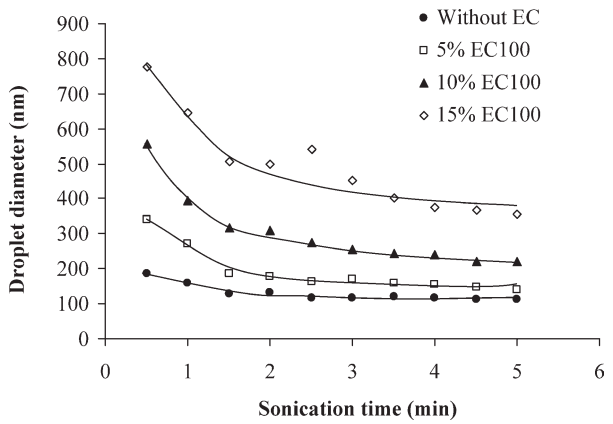

FIGURE 1 Droplet diameter versus sonication time for EC100-containing acrylic miniemulsions. The lines are guides for the eye. See Table 2 for experimental details.

Synthesis of EC-Based Hybrid Latexes Through Miniemulsion Polymerization

Effect of EC Content and EC Viscosity on Droplet Nucleation and Latex Stability

In a first series of experiments, we studied the effect of EC100 on droplet nucleation and latex particle formation, keeping in mind the high viscosity of the dispersed phase for high EC100 contents. Table 2 reports the final monomer conversion for each experiment whereas Figure 2 displays the evolution of particle size with conversion. In the absence of EC or for a low-amount of EC (typically 5 wt %), the system shows the expected features of miniemulsion polymerization that is to say a constant evolution of particle diameter with conversion indicating efficient droplet nucleation. However, when increasing the EC100 content to 10 and 15 wt %, the particle diameter decreased with increasing conversion, whereas the monomer conversion leveled off. In addition, some coagulum, the amount of which was not quantified at this stage, was formed in both cases. Note that some

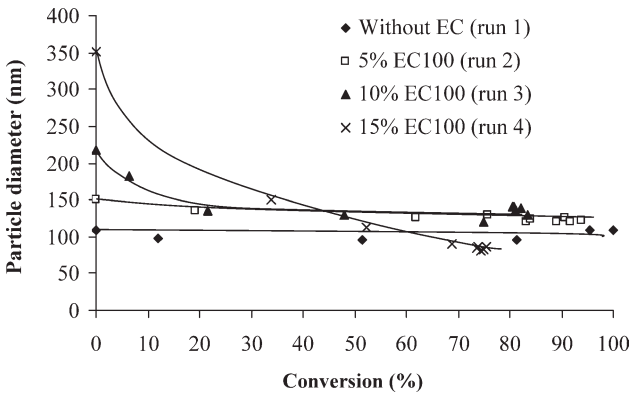

FIGURE 2 Evolution of particle size versus conversion during miniemulsion polymerization of MMA and BA in the presence of increasing EC100 contents. The lines are guides for the eye.

coagulum was also observed for 5 wt % of EC but in lower proportions.

These results can be interpreted as follows. The interfacial area developed by the large droplets formed in presence of a high amount of EC is too low to ensure efficient capture of the growing oligoradicals. Given the relatively high solubility of MMA in water (15 $g \cdot L^{-1}$), homogeneous nucleation is thus likely to occur, giving rise to the formation of small particles stabilized by surfactant. As the monomer diffuses from the large droplets to these secondary-nucleated particles, EC would be expelled out of the original miniemulsion droplets, as it cannot transport through the water phase. This would result in latex coagulation, as there would not be enough surfactant to stabilize both the newly created particles and the EC polymer. As a direct consequence, the formation of coagulum leads to underestimated monomer conversions. The higher the EC content, the less stable the latex suspension and, thus the lower the monomer conversion at the plateau.

As mentioned above, the large droplet size is the result of high viscosity of the dispersed phase. Therefore, in an attempt to decrease the droplet size while maintaining reasonable EC contents, the lower-viscosity EC grade (i.e., EC10) was evaluated under otherwise identical experimental conditions. In this new series of experiments, the amount of coagulum (expressed in weight fraction of the total amount of solid produced during the polymerization) was determined experimentally by weighing the solid residue. Although the use of EC10, that has a lower viscosity than EC100, gave rise to lower droplet sizes (see run 5 in Table 2), the resulting latex still contained some amount of coagulum. In this case (Fig. 3), the particle size first increased to 250 nm and then decreased to values lower than the size of the parent miniemulsion, whereas concurrently, the monomer conversion leveled up to around 70%. In addition, it is worth noting that the transitory increase in size was concomitantly accompanied with a decrease in polymerization rate.

The increase in particle size at low conversion indicates that the droplets were unstable and coalesced during the early stages of polymerization. Different reasons may explain why the system was not stable in the presence of EC10. First, EC and the polymer matrix may be not compatible with each other, thus inducing phase separation inside the monomer swollen particles. Indeed, EC solubility inside the particles would decrease, as the polymerization proceeds ultimately leading to phase separation and coalescence of the nucleated particles. In addition, EC is known to be able to reduce the interfacial tension of water-in-oil emulsion.[34] EC is therefore expected to be more compatible with the aqueous phase than with the polymer. EC migration at the oil/water interface may emphasize the phase separation process. Therefore, as before for EC100, EC10 is likely to be excluded from the latex particles upon polymerization. This last hypothesis was supported by TEM observation of the hybrid latex after polymerization, which clearly shows the presence of free EC displaying an elongating rod-like shape, together with spherical EC-free latex particles [Fig. 4(b)].

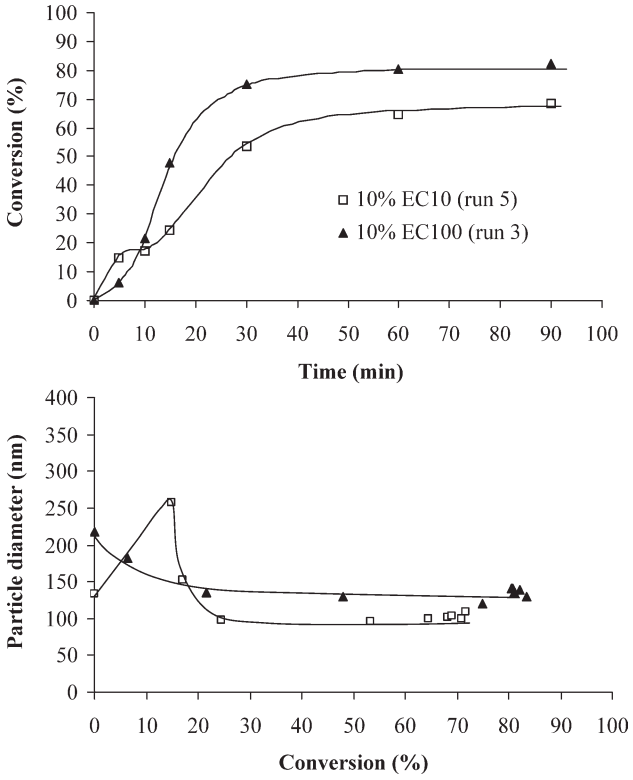

FIGURE 3 Evolution of monomer conversion and particle size during miniemulsion polymerization of MMA and BA in the presence of 10 wt % of EC10 (run 5) or EC100 (run 3). The lines are guides for the eye.

To support the assumption of EC preferential location at the oil/water interface, we determined the amount of SDS present in the continuous phase for different systems (Table 5). As most of the surfactant is adsorbed onto the surface of the droplets, which exhibit a high interfacial area, the SDS concentration in the aqueous phase is expected to be lower than the CMC. This was confirmed by measuring the conductivity of the miniemulsions for the two grades of EC. Table 5 also shows that for a given EC grade, the amount of free SDS increases with increasing EC content in agreement with the increase in droplet size. In addition, for the same initial amount of EC, the droplet size is significantly lower in the case of EC10, whereas, at the same time, the concentration of SDS in the aqueous phase is higher. This suggests that EC10 is preferentially located at the interface of the monomer droplets with water, thus displacing part of the SDS molecules. Despite the fact that EC100 has higher viscosity and molar mass, and probably less affinity for the water phase than EC10, the above scenario also holds for this EC grade and may account for the poor latex stability also observed in this case.

Addition of a Crosslinker

It is well-known that the use of a crosslinker leads to the formation of a polymer network of limited mobility that might decrease the extent of phase separation.[35] To prevent expulsion of EC out of the monomer droplets and physically

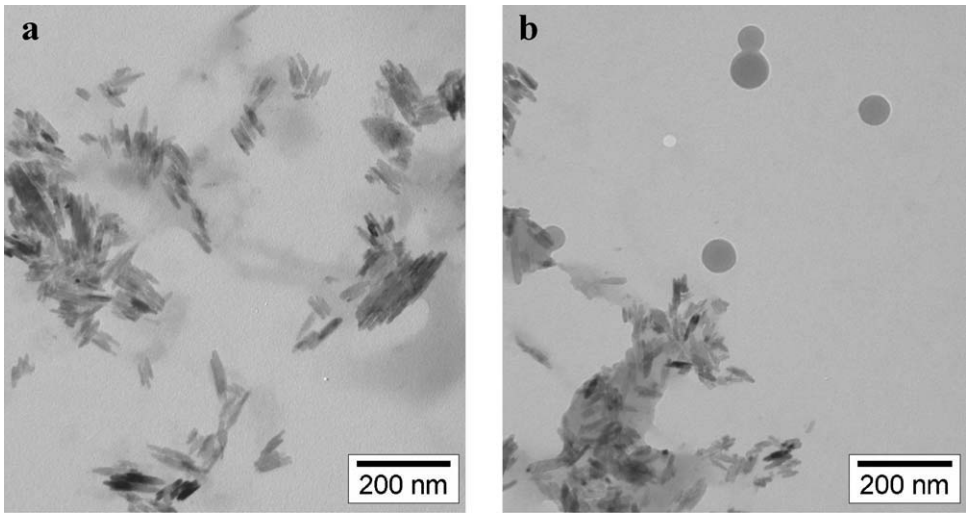

FIGURE 4 TEM pictures of EC10-containing (a) miniemulsion and (b) latex (EC content = 10 wt %, run 5). Note that for the miniemulsion, only EC is visible because the droplets disappear upon TEM observation.

hold EC inside the particles, the next series of experiments was thus performed with triethylene glycol dimethacrylate (TEGDMA) as a crosslinking agent using 4.7 wt % of TEGDMA with respect to the monomers/EC mixture (run 6, Table 2). The amount of coagulum was effectively lowered but was still too high to be acceptable (26 wt % versus 38 wt % without TEGDMA). In addition, the evolution of particle size with conversion followed almost the same trend with or without TEGDMA (i.e., the particle size first increased and then decreased) (Fig. 5). In conclusion, the sole use of TEGDMA was not able to prevent EC diffusion and improve latex stability.

Another effective means of keeping EC inside the particles and decrease the extent of phase separation would be to chemically graft EC to the polymer chains constituting the particles. Indeed, many studies report in the literature the formation of graft copolymers from the backbone of cellulose and cellulosic derivatives using radical initiators.[36–40] APS being located in the aqueous phase, the formation of radicals on the EC backbone may not be efficient. This is why the next series of experiments was performed with an organo-soluble initiator, the LPO. Effectively, when LPO was used as initiator and TEGDMA as crosslinker, the obtained latex (run 7, Table 2) was perfectly stable (no coagulum) with 100% conversion. LPO being closely located to EC, it is thus very likely that EC was implicated in the free radical process to form graft copolymers. Note that in this case, particle size increases with increasing conversion indicating the occurrence of coalescence. In other words, we have created fewer particles than the number of monomer droplets initially present in the reactor (Fig. 5). A similar discrepancy between the initial number of droplets and the final number of latex particles has already been reported in the literature for miniemulsion polymerizations performed in the presence of oil-soluble initiators.[41,42]

What is worth to be noted is the particular morphology of the particles [Fig. 6(a)] even in the absence of EC [run 8, Fig. 6(b)]. Indeed, the majority of the particles (which are polydisperse in size) seem to be constituted of two phases with different electron densities (one dense, the other not) leading to a half moon-like morphology. This morphology is likely the result of an interplay of thermodynamic and kinetic factors operating during the polymerization process. Indeed, the reactivity ratios for MMA/BA copolymerization ($r_{MMA} = 2.55 \pm 0.35$; $r_{BA} = 0.36 \pm 0.08$[43]) indicate that MMA is more reactive than BA and thus preferentially incorporated leading to a compositional drift. In addition, the presence of the crosslinker TEGDMA whose reactivity is

TABLE 5 Droplet Size, Conductivity, and Concentration of Free SDS as a Function of EC Grade and EC Content for EC-Containing Miniemulsions[a]

EC Grade	EC Content (%)	Droplet Size (nm)	Conductivity ($S \cdot cm^{-1}$)	$[SDS]_{free}$ ($g \cdot L^{-1}$)[b]
EC10	5	105	778	1.68
EC10	10	143	909	1.98
EC10	15	174	1,031	2.26
EC100	5	145	735	1.58
EC100	10	225	864	1.87

[a] Please note that the slight differences which may be observed in term of particle size between this series of experiments and similar recipes used for subsequent polymerization and detailed in Table 2 are within the measuring error range.

[b] CMC value determined for SDS in an APS/water solution = 2.36 $g \cdot L^{-1}$.

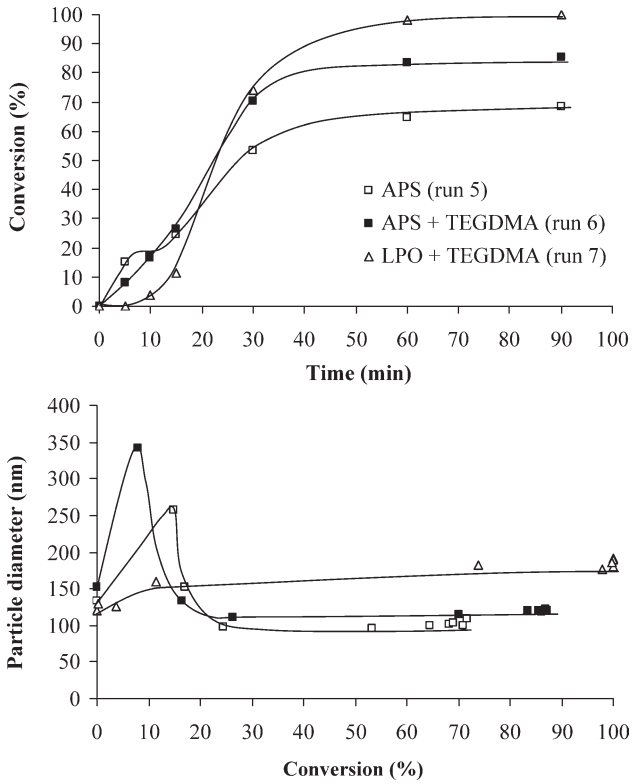

FIGURE 5 Effect of the addition of a crosslinker on the evolution of monomer conversion and particle size during miniemulsion polymerization of MMA and BA initiated by APS or LPO in the presence of 10 wt % of EC10. The lines are guides for the eye.

likely similar to that of MMA, will lead to the formation of a PMMA-rich and crosslinked phase. Because of the limited swelling of this phase by the monomer(s), polymerization will eventually lead to asymmetrical particles with a PBA-rich phase (with a low electron density) according to mechanisms likely similar to those depicted by Sheu et al.[44] and Mock et al.[45] In these works, it was reported that heating monomer-swollen crosslinked polymer seed caused the phase separation of the monomer from the seed in the form of a nonuniform bulge, which upon polymerization resulted in the formation of asymmetrical particles. Taking these considerations into account, it though remains quite difficult to predict which phase (PMMA or PBA) would be enriched in EC. What could be drawn from TEM images was that no free EC was never detectable on any TEM images [Fig. 6(b)]. This, together with the absence of coagulum, would indicate an efficient encapsulation of EC inside the particles. The fact that EC crystals could not be distinguished could be explained by the reactivity of radical initiators toward cellulose and its derivative. Indeed, the use of oxygen-centered radicals has been reported to strongly degrade cellulosic backbone.[20,38] The addition of a radical initiator such as LPO could effectively lead to the formation of EC-based graft copolymers in the presence of vinyl monomer as shown in Scheme 1.

To support this assumption, copolymerization of MMA/BA was carried out in toluene (67 wt % of solvent) without or with EC (10 wt % of EC10). The polymerization performed in the presence of EC resulted in a lower molar mass providing further evidence of EC implication in the free radical process. Indeed, the molar mass was unchanged when EC was simply blended with the copolymer.

The combined use of TEGDMA and LPO giving satisfactory results in terms of both colloidal stability and monomer conversion, the EC10 content was then increased from 10 to 15 wt % (run 9). The reaction behaved in a very similar way at the beginning of the polymerization but the latex then became unstable. This loss of stability is likely related to the amount of EC used in these experiments leading to the formation of droplets of high internal viscosity. Increasing the amount of TEGDMA for a fixed amount of EC (8.4 and 17 wt %, for runs 10 and 11, respectively) did not improve the latex colloidal stability. Moreover, the higher the amount of TEGDMA, the lower was the final conversion. It is possible that the high crosslinking density of the latex particles might limit their swelling capacity by the monomer.

The conditions described above (LPO, 10 wt % EC, and 4.7 wt % TEGDMA) were then applied to EC100 grade (run 12).

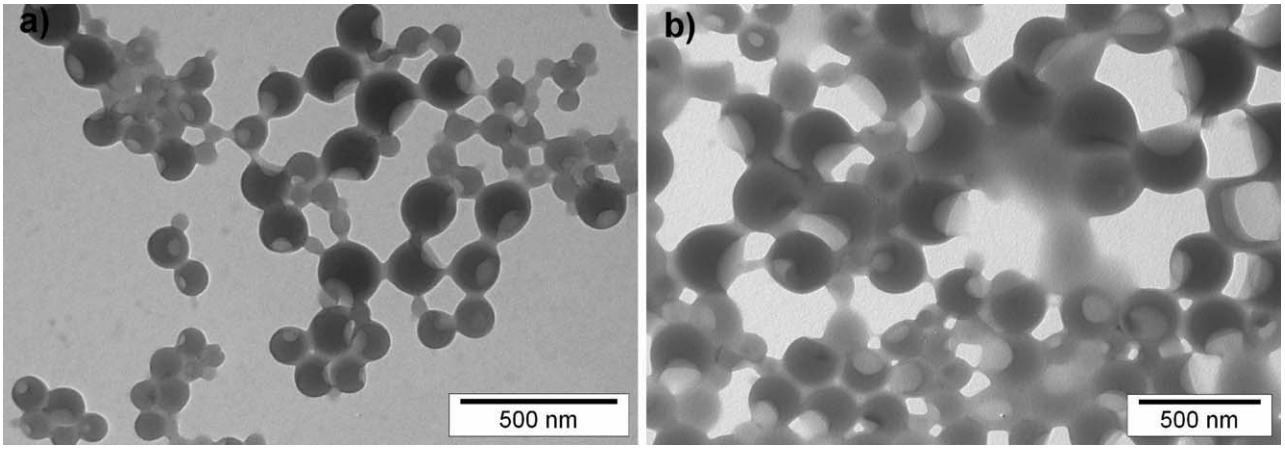

FIGURE 6 TEM pictures of LPO/TEGDMA-based systems (a) without EC (run 8) and (b) with 10 wt % of EC 10 (run 7).

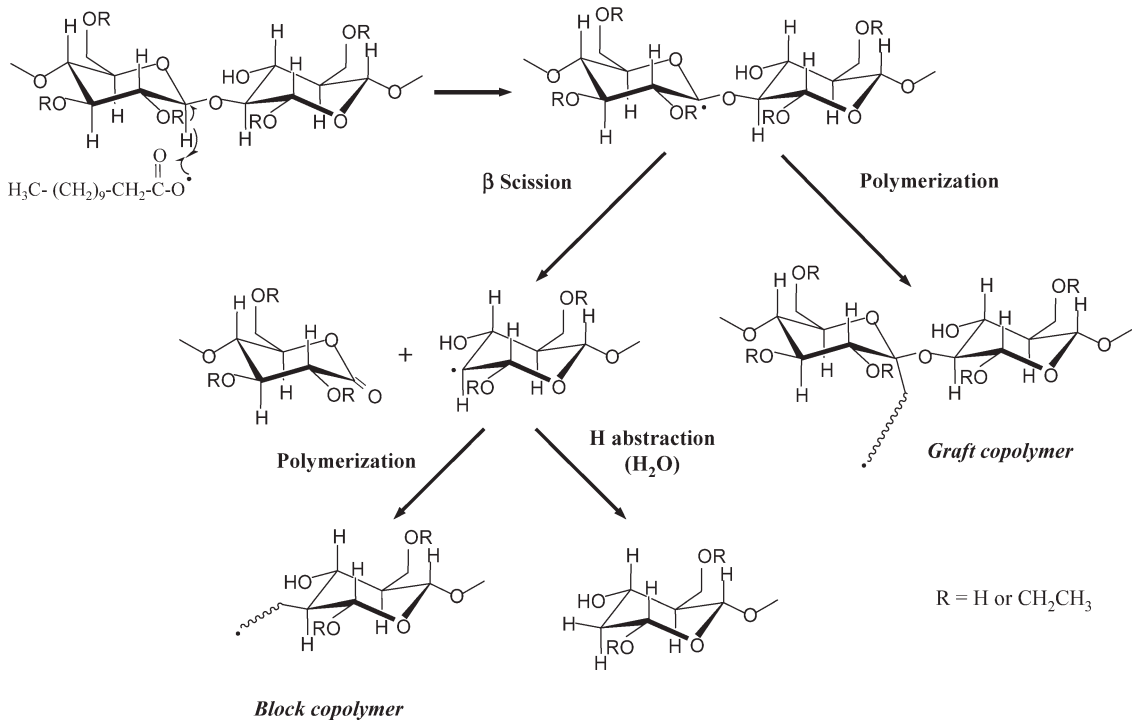

SCHEME 1 Mechanism for free-radical grafting and degradation of EC, adapted from the one proposed in reference 20.

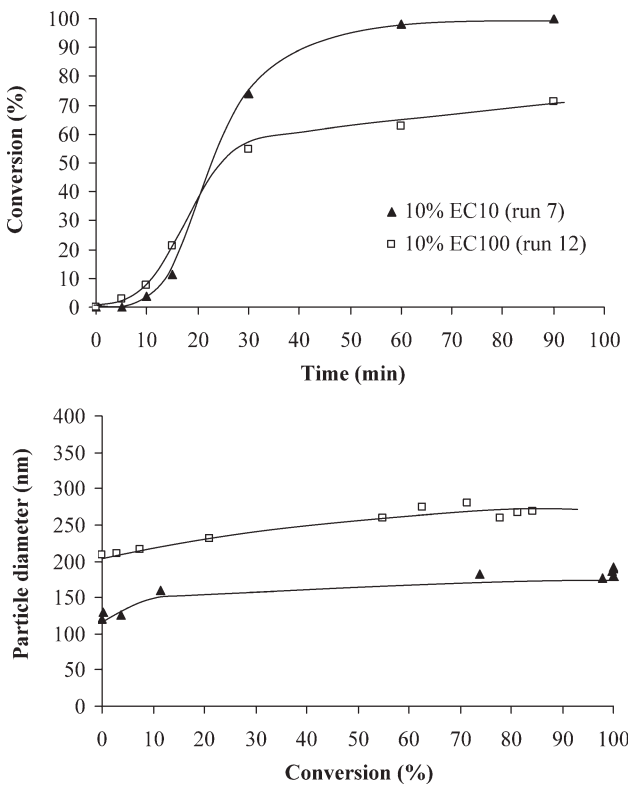

FIGURE 7 Evolution of monomer conversion and particle size during miniemulsion polymerizations of MMA and BA initiated by LPO in the presence of 4.7 wt % of TEGDMA and 10 wt % of EC10 (run 7) or EC100 (run 12). The lines are guides for the eye.

Similarly to the APS-initiated system, the droplet size is higher when the viscosity of EC is increased. Despite the presence of TEGDMA, the obtained latex was not stable and 13 wt % of coagulum was obtained that can account for the limiting conversion observed in this case (Fig. 7). As seen in Figure 8, the particle size distribution is larger than the EC10-based latex in agreement with DLS measurement (Table 2), whereas the particles exhibit a similar half-moon morphology.

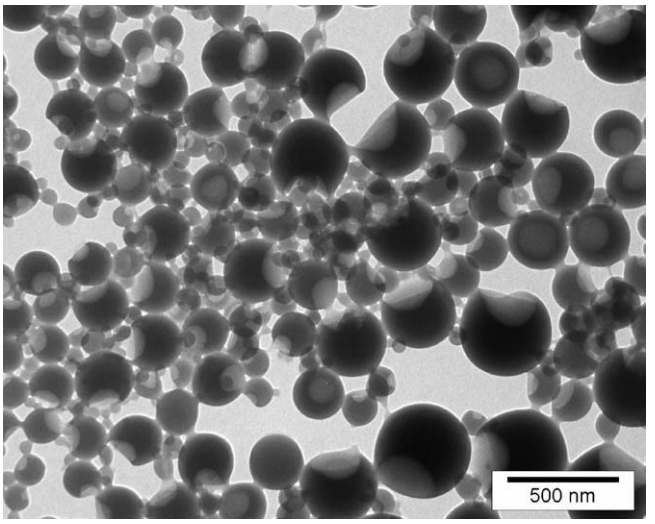

FIGURE 8 TEM image of EC100-based latex particles elaborated with LPO as initiator and TEGDMA as crosslinker (run 12).

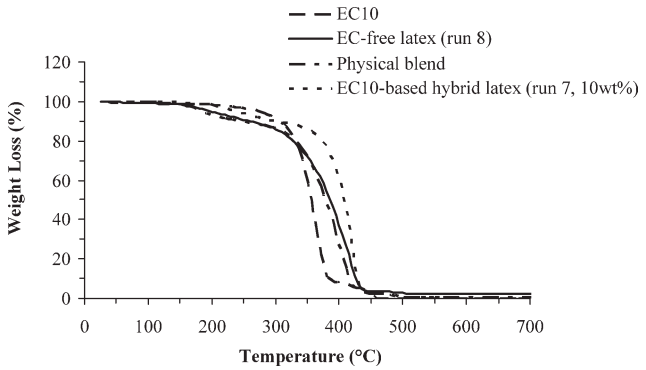

FIGURE 9 TGA curves of EC10 powder, an EC-free latex (run 8), a physical blend of EC10 powder (10 wt %) and an EC-free latex (run 8), and EC10-based hybrid latex (10 wt %, run 7).

As evidenced by all the results discussed above, the synthesis of colloidally stable latexes incorporating a high amount of EC is not straightforward. We however succeeded in the formation of stable acrylic latexes incorporating up to 10 wt % of low-viscosity EC10. The film properties of these latexes have then been studied and compared with those of physical blends containing the same amount of EC. The results are presented below.

Thermomechanical Properties of EC-Based Hybrid Latexes

This section will focus on the latex obtained in the presence of TEGDMA, LPO, and 10 wt % of EC 10 (run 7). The properties of the films obtained from this latex will be compared with those of EC alone, of the film formed from an EC-free latex (run 8, referred to as the blank matrix) and/or of a physical blend obtained by mixing 10 wt % of EC10 with the blank matrix.

Differential Scanning Calorimetry

The film formed from the hybrid latex (run 7), the blank matrix, and the physical blend were first characterized using DSC. The blank matrix shows only one T_g at 17.5 °C corresponding to the onset temperature of the phenomenon. No clear shift of the T_g value was noticed for the physical blend (T_g around 17 °C). In contrast, for the hybrid latex, a 3 °C shift toward lower temperature was observed. This result supports the assumption of latex hybridization and chemical incorporation of EC polymers by free radical polymerization as represented in Scheme 1.

Thermal Gravimetric Analysis

TGA experiments were then performed on EC and the different films (Fig. 9). For EC, the obtained curve is in agreement with the literature.[46] The thermal degradation of the acrylic polymer starts at around 190 °C and is almost complete at 450 °C (run 8). Given the low weight fraction of EC10, the curve corresponding to the physical blend is very close to that of the acrylic polymer with a degradation beginning at 181 °C. It is worth noting that this curve corresponds to the weighted summation of the EC10 curve and of the EC-free latex curve. In contrast, the degradation is significantly delayed in the case of the hybrid latex (run 7: 218 °C) indicating that the presence of EC provides improved thermal resistance to the hybrid film. The increased copolymer thermal stability is probably related to the modification of the copolymer composition in the presence of EC, which will be confirmed by DMA analysis. Indeed, the thermal degradation of copolymers is known to be strongly dependent on their compositions.[47]

Dynamic Mechanical Analysis

DMA experiments were performed on the different films to characterize the influence of EC on their viscoelastic properties. Figure 10 presents the comparison between the films obtained from the EC-free latex, the physical blend, and the EC10-based hybrid latex.

DMA curve of the physical blend incorporating 10 wt % of EC is very similar to that of the blank matrix. The main relaxation, indicated by a large modulus drop and a tanδ peak, occurs at the same temperature for both materials; the loss factor peak is located at $T = 42$ °C. This confirms the DSC results, which suggested that the mixing of the matrix with 10 wt % of EC10 does not modify the glass transition temperature. The addition of EC10 only slightly increases the modulus value. This increase vanishes at temperature above 90 °C, that is, when the temperature approaches that of the glass transition temperature of EC10. For the hybrid material, the G' decrease associated with Tα starts earlier, observation which is also in agreement with the DSC measurements. Furthermore, in that case, a second peak is observed at temperature around 107 °C. These results can be

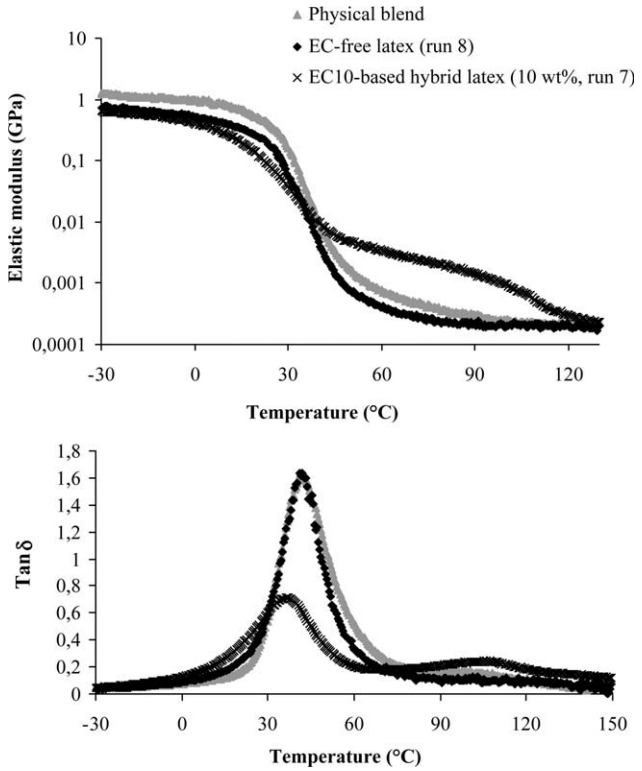

FIGURE 10 DMA curves of EC-free latex (run 8), of physical blend of latex and EC10 powder (10 wt %) and of EC10-based hybrid latex (10 wt %, run 7).

associated with the composition drift discussed above. The main relaxation shift toward lower temperature would be because of a polymer phase poorer in MMA units. Within this assumption, the second peak, at temperature around 107 °C, could be attributed to a PMMA enriched phase, because it is well known that the PMMA phase has a relaxation temperature in this temperature region. However, if the peak at 107 °C is related to a composition drift of the copolymer, it should also be present in the DMA curve of the EC-free latex which is not the case. One could also argue that the peak at 107 °C is because of the EC α relaxation. Indeed, this one has clearly been observed at this temperature in EC/acrylic blends when the EC contents are above 30% (DMA results not presented here). However, in this case, the EC content is much lower than 30% (i.e., 10 wt %), and the peak is actually located at temperature slightly lower than the EC relaxation temperature, which is around 120 °C. At last, it must be noted that the presence of EC in the hybrid leads to a large increase of the modulus at temperature between 30 and 100 °C. Such an increase of the modulus by a factor 10 is too high to be attributed to the reinforcement by isolated EC domains. Moreover, no EC domains could be identified in the TEM picture of the hybrid latex [Fig. 6(b)], while there is no significant reinforcement of the modulus in the glass transition region (before the main relaxation). Thus, it can be proposed that the EC10 molecules have been intimately linked to the polymer chains, giving birth to a second phase with a glass transition temperature slightly above 100 °C. Given the large modulus at temperature below this T_g, this phase likely percolated, creating a network rigid at temperature below its glass transition temperature.

CONCLUSIONS

A series of EC-containing hybrid latexes were prepared by reacting simultaneously EC, MMA, and BA in miniemulsion polymerization. It was shown that the droplet size and latex stability were strongly dependent on EC viscosity and EC content. When APS was used as initiator, the higher the EC content and EC viscosity, the less stable were the latex suspensions. This was attributed to EC expulsion out of the latex particles upon polymerization because of phase incompatibility between EC and the acrylic polymer. Stable hybrid latexes free of any coagulum and containing up to 10 wt % of low-viscosity EC could be successfully obtained by using a crosslinker that physically retained EC inside the latex particles, and an oil-soluble initiator capable of undergoing chemical graft reactions with the cellulose backbone increasing thereby chemical compatibility. The films issued from the hybrid latex showed superior thermal and mechanical properties compared with the EC-free latex film and to the film made from a physical blend of EC and EC-free latex. It was proposed that in situ grafting of acrylic radicals to EC led to the formation of an EC-based hybrid polymer phase that formed a rigid percolating network at temperatures below its glass transition temperature.

C. Graillat and P. Y. Dugas are acknowledged for their help in viscosity and conductimetry measurements.

REFERENCES AND NOTES

1 (a) Klemm, D.; Philipp, B.; Heinze, T.; Heinze, U.; Wagenknecht, W. Comprehensive Cellulose Chemistry; Vol. 2, Wiley-VCH: Weinheim, 1998; p 220; (b) Klemm, D.; Heublein, B.; Fink, H. P.; Bohn, A. Angew Chem Int Ed Engl 2005, 44, 3358–3393.

2 Abdel-Razik, E. A. J Photochem Photobiol A Chem 1993, 73, 53–58.

3 Yuan, W.; Yuan, J.; Zhang, F.; Xie, X. Biomacromolecules 2007, 8, 1101–1108.

4 Tang, X. D.; Gao, L. C.; Fan, X. H.; Zhou, Q. F. J Polym Sci Part A: Polym Chem 2007, 45, 1653–1660.

5 Shen, D. W.; Yu, H.; Huang Y. J Polym Sci Part A: Polym Chem 2005, 43, 4099–4108.

6 Li, Y.; Liu, R.; Liu, W.; Kang, H.; Wu, M.; Huang, Y. J Polym Sci Part A: Polym Chem 2008, 46, 6907–6915.

7 Kang, H. L.; Liu, W. Y.; He, B. Q.; Shen, D. W.; Ma, L.; Huang, Y. Polymer 2006, 47, 7927–7934.

8 Aggour, Y. A. J Mater Sci 2000, 35, 1623–1627.

9 Lim, D. W.; Song, K. G.; Yoon, K. J.; Ko, S. W. Eur Polym Materl 2002, 38, 579–586.

10 Hutchings, D.; Clarson, S.; Sakr, A. Int J Pharm 1994, 104, 203–213.

11 Wallström-Wennerstrand, A.; Olsson, M.; Jaernström, L.; Koschella, A.; Fenn, D.; Heinze, T. J Colloid Interf Sci 2008, 327, 51–57.

12 Yang, C. Y.; Tsay, S. Y.; Tsiang, R. C. C. J Microencapsul 2001, 18, 223–236.

13 Choudhury, P. K.; Kar, M. J Microencapsul 2009, 26, 46–53.

14 Palmieri, G. F.; Grifantini, R.; Di Martino, P.; Martelli, S.; Drug Dev Ind Pharm 2000, 26, 1151–1158.

15 Gallardo, V.; Morales, M. E.; Ruiz, M. A.; Delgado, A. V. Eur J Pharm Sci 2005, 26, 170–175.

16 Gallardo, V.; Morales, M. E.; López-Viota, J.; Durán, J. D. G.; Ruiz, M. A. J Appl Polym Sci 2006, 102, 847–851.

17 Vanderhoff, J. W.; El-Aasser, M. S.; Ugelstad, J. U.S. Patent 4,177,177, 1979.

18 Thioune, O.; Briançon, S.; Devissaguet, J. P.; Fessi, H. Drug Dev Res 2000, 50, 157–162.

19 Arias, J. L.; López-Viota, M.; Ruiz, M. A.; López-Viota, J.; Delgado, A. V. Int J Pharm 2007, 339, 237–245.

20 Annable, T.; Gray, I.; Lovell, P. A.; Richards, S. N.; Satgurnathan, G. Prog Colloid Polym Sci 2004, 124, 159–163.

21 Janssen, B. J. W.; Kroon, G.; Kruythoff, D.; Salomons, W. G. WO Patent 014,357 1996.

22 Lelu, S.; Novat, C.; Graillat, C.; Guyot, A.; Bourgeat-Lami, E. Polym Int 2002, 52, 542–547.

23 Joumaa, N.; Lansalot, M.; Théretz, A.; Elaissari, A.; Sukhanova, A.; Artemyev, M.; Nabiev, I.; Cohen, J. H. M. Langmuir 2006, 22, 1810–1816.

24 Joumaa, N.; Toussay, P.; Lansalot, M.; Elaissari, A. J Polym Sci Part A: Polym Chem 2008, 46, 327–340.

25 Costoyas, A.; Ramos, J.; Forcada, J. J Polym Sci Part A: Polym Chem 2009, 47, 935–948.

26 Goikoetxea, M.; Minari, R. J.; Beristain, I.; Paulis, M.; Barandiaran, M. J.; Asua, J. M. J Polym Sci Part A: Polym Chem 2009, 47, 4871–4885.

27 (a) Koppel, D. E. J Chem Phys 1972, 57, 4814–4820; (b) International Standard ISO 13321. Methods for determination of particle size distribution. Part 8: Photon Correlation Spectroscopy, International Organization for Standardization (ISO) 1996.

28 Erdem, B.; Sully, Y.; Sudol, E. D.; Dimonie, V.; El-Aasser, M. S. Langmuir 2000, 16, 4890–4895.

29 Etienne, S.; Cavaille, J. Y.; Perez, J.; Point, R.; Salvia, M. Rev Sci Instrum 1982, 53, 1261–1266.

30 Blythe, P. J.; Morrison, B. R.; Mathauer, K. A.; Sudol, E. D.; El-Aasser, M. S. Langmuir 2000, 16, 898–904.

31 do Amaral, M.; Bogner, A.; Gauthier, C.; Thollet, G.; Jouneau, P.-H.; Cavaille, J. Y.; Asua, J. M. Macromol Rapid Commun 2005, 26, 365–368.

32 Jahanzad, F.; Karatas, E.; Saha, B.; Brooks, B.-W. Colloids Surf A 2007, 302, 424–429.

33 Mabille, C.; Leal-Calderon, F.; Bibette, J.; Schmitt, V. Europhys Lett 2003, 61, 708–714.

34 Melzer, E.; Kreuter, J.; Daniels, R. Eur J Pharm Biopharm 2003, 56, 23–27.

35 Luo, Y.; Zhou, X. J Polym Sci Part A: Polym Chem 2004, 42, 2145–2154.

36 Nishioka, N.; Kosai, K. Polym J 1981, 13, 1125–1133.

37 Nishioka, N.; Minami, K.; Kosai, K. Polym J 1983, 15, 591–596.

38 Abdel-Razik, E. A. Polymer 1990, 31, 1789–1744.

39 Aggour, Y. A.; Abdel-Razik, E. A. Eur Polym J 1999, 35, 2225–2228.

40 Wang, L.; Dong, W.; Xu, Y. Carbohydr Polym 2007, 68, 626–636.

41 Asua, J. M.; Rodriguez, V. S.; Sudol, E. D.; El Aasser, M. S. J Polym Sci Part A: Polym Chem 1989, 27, 3569–3587.

42 Graillat, C.; Guyot, A. Macromolecules 2003, 36, 6371–6377.

43 Buback, M.; Feldermann, A.; Barner-Kowollik, C.; Lacík, I. Macromolecules 2001, 34, 5439–5448.

44 Sheu, H. R.; El-Aasser, M. S.; Vanderhoff, J. W. J Polym Sci Part A: Polym Chem 1990, 28, 629–651.

45 Mock, E. B.; De Bruyn, H.; Hawkett, B. S.; Gilbert, R. G.; Zukoski, C. F. Langmuir 2006, 22, 4037–4043.

46 Chen, K.; Lü, Z.; Ai, N.; Huang, X.; Zhang, Y.; Ge, X.; Xin, X.; Chen, X.; Su, W. Solid State Ionics 2007, 177, 3455–3460.

47 Konaganti, V. K.; Madras, G. Ind Eng Chem Res 2009, 48, 1712–1718.